FOXO3a-SIRT6 axis suppresses aerobic glycolysis in melanoma

ZHEN DONG[1-4], JIE YANG[1-4], LIN LI[1-4], LI TAN[1-4], PENGFEI SHI[1-4], JIAYI ZHANG[1-4], XI ZHONG[1-4], LINGJUN GE[1-4], ZONGHUI WU[5] and HONGJUAN CUI[1-4]

[1]State Key Laboratory of Silkworm Genome Biology, Institute of Sericulture and Systems Biology, [2]Cancer Center, Medical Research Institute, [3]Engineering Research Center for Cancer Biomedical and Translational Medicine, [4]Chongqing Engineering and Technology Research Center for Silk Biomaterials and Regenerative Medicine, [5]Hospital of Southwest University, Southwest University, Chongqing 400716, P.R. China

Received June 11, 2019; Accepted December 10, 2019

DOI: 10.3892/ijo.2020.4964

Abstract. Melanoma, the most aggressive human skin tumor, has a very short survival time, and there are currently no effective treatments. Alterations in cell metabolism, such as enhanced aerobic glycolysis, have been identified as hallmarks of cancer cells. In the present study, bioinformatics studies using online databases revealed that *FOXO3a* expression was lower in melanoma tissues compared with normal tissues and nevus. Additionally, Kaplan-Meier analysis showed that high expression of *FOXO3a* predicted an improved prognosis for patients with melanoma. Furthermore, Pearson correlation analysis indicated that the expression of *FOXO3a* was positively correlated with *SIRT6* expression and negatively correlated with the expression levels of a number of glycolysis-associated genes. Chromatin immunoprecipitation and luciferase assays showed that FOXO3a was enriched in the *SIRT6* promoter region and promoted its transcription. Then, SIRT6 was overexpressed in FOXO3a-knockdown MV3 cells and downregulated in FOXO3a-overexpressing MV3 cells by using lentivirus-mediated stable infection. The results showed that SIRT6 knockdown or overexpression rescued the effects of FOXO3a overexpression or knockdown, respectively, on glycolysis, as determined by glucose uptake, glucose consumption and lactate production assays, the expression of glycolytic genes and glucose stress flux tests. SIRT6 overexpression also suppressed FOXO3a knockdown-induced tumor growth in a mouse model. The present findings indicated that the FOXO3a-SIRT6 regulatory axis inhibited glucose metabolism and tumor cell proliferation in melanoma, and provided novel insight into potential therapeutic strategies to treat this disease.

Correspondence to: Professor Hongjuan Cui, State Key Laboratory of Silkworm Genome Biology, Institute of Sericulture and Systems Biology, Southwest University, 2 Tiansheng Road, Beibei, Chongqing 400716, P.R. China
E-mail: hcui@swu.edu.cn

Dr Zonghui Wu, Hospital of Southwest University, Southwest University, 2 Tiansheng Road, Beibei, Chongqing 400716, P.R. China
E-mail: wuzh@swu.edu.cn

Key words: forkhead box O3, sirtuin 6, aerobic glycolysis, melanoma, glucose metabolism

Introduction

Melanoma is the most lethal skin cancer; it is responsible for the vast majority of cutaneous cancer deaths globally, even though it only accounts for ≤5% of all cutaneous carcinomas (1). In the early stages, melanoma can be treated with surgical resection; however, once metastasis occurs, it is resistant to conventional radio- and chemotherapy, and is extremely difficult to treat (2). Therefore, it is urgent to acquire an improved understanding of the properties of melanoma in order to develop effective treatment regimens.

Alterations in cellular metabolism have been recognized as hallmarks of malignant tumors (3,4). Aerobic glycolysis, also termed the Warburg effect, is one of the most important hallmarks in the reprogramming of cancer metabolism via upregulated glycolytic enzymes and activated regulatory factors, including oncogenes (p53, c-Myc and K-Ras), essential signaling pathways [PI3K/Akt, liver kinase B1/AMP kinase and hypoxia-inducible factor 1 (HIF1) signaling pathways] and epigenetic regulators such as sirtuins (SIRTs) (5-8). Importantly, aerobic glycolysis has been demonstrated to provide a specific microenvironment to promote unconstrained proliferation and invasion (9). Therefore, controlling cellular metabolism may be a potential targeted therapeutic strategy to treat malignant tumors such as melanoma.

Forkhead box O (FOXO) transcription factors, including FOXO1, FOXO3a, FOXO4 and FOXO6, which are conserved from *Caenorhabditis elegans* to mammals, serve pivotal roles in multiple cellular processes, such as cell cycle progression, apoptotic cell death, DNA repair, oxidative stress, epithelial-mesenchymal transition and cellular metabolism (10-13). FOXO3a, an important member of the FOXO family, participates into the modulation of cell growth in multiple tumors, including glioblastoma (14), prostate cancer (15), lung adenocarcinoma (16), ovarian cancer (17), colorectal cancer (18) and Hodgkin's lymphoma (19). It was reported that FOXO3a is also an important regulator of cellular metabolism in tumors; for example, FOXO3a regulates reactive oxygen metabolism by

inhibiting mitochondrial gene expression in colon cancer (20). Additionally, FOXO3a has been shown to regulate multiple cellular process, including cell survival, apoptosis (21-23), migration and invasion (24) in melanoma. However, the role of FOXO3a in the regulation of cellular metabolism in melanoma has never been explored.

The present study aimed to elucidate the role of the FOXO3a-SIRT6 axis in the interplay between cellular metabolism and tumor progression, thereby providing novel insight into potential melanoma treatment strategies. In the present study, it was observed that FOXO3a inhibited aerobic glycolysis by targeting the promoter of *SIRT6* and promoting its transcription, thereby inhibiting the expression of a cluster of glycolysis-associated genes.

Materials and methods

Cell lines and reagents. The MV3 melanoma cell line was obtained from the Third Military Medical University, and cultured in RPMI-1640 (Thermo Fisher Scientific, Inc.) supplemented with 10% fetal bovine serum (FBS; Thermo Fisher Scientific, Inc.) and 1% penicillin-streptomycin (P/S; Invitrogen; Thermo Fisher Scientific, Inc.). PIG1 normal melanocytes, and SK-MEL-28 and A375 melanoma cell lines were purchased from the American Type Culture Collection (ATCC) and cultured in Dulbecco's Modified Eagle's minimum essential medium (DMEM, Thermo Fisher Scientific, Inc.) supplemented with 10% FBS and 1% P/S. All cells were cultured at 37˚C in a 5% CO_2 incubator (Sanyo). 2-Deoxy-2-[(7-nitro-2,1,3-benzoxadiazol-4-yl) amino]-D-glucose (2-NBDG; cat. no. N13195) was purchased from BD Biosciences. MTT (cat. no. M2128) and DMSO (cat. no. D2650) were purchased from Sigma-Aldrich (Merck KGaA).

Reverse transcription-quantitative PCR (RT-qPCR). RNA was extracted from cells following specific treatments using RNAiso Plus (Takara Bio, Inc.), trichloromethane (Sigma-Aldrich; Merck KGaA), isopropanol (Shanghai Dingguo Biological Technology Co., Ltd.) and 75% ethanol (Shanghai Dingguo Biological Technology Co., Ltd.) according to the manufacturer's protocol. cDNA was obtained from 2 μg RNA/sample using a GoScript™ Reverse Transcriptase kit (cat. no. A5001; Promega Corporation) according to the manufacturer's protocols. Then, RT-qPCR was performed to analyze the mRNA expression of genes using a LightCycler® 96 Instrument (Roche Diagnostics). Promega GoTaq® qPCR Master Mix (cat. no. A6001; Promega Corporation) was used. The PCR reaction conditions were as follows: 95˚C pre-denaturation for 10 min; then, 45 cycles of 95˚C for 15 sec, 60˚C for 30 sec and 72˚C for 30 sec; then, 95˚C for 10 sec, 60˚C for 1 min, 97˚C for 1 sec and 37˚C for 30 sec. Results were calculated via the $2^{-\Delta\Delta Cq}$ method (25) with *ACTB* expression used as the internal control (Cq value was used instead of Ct value in this study). The primers, which were also used in a previous study (14), were presented in Table I.

Vector construction and stable transfection. Short hairpin RNA (shRNA) sequences were designed using siRNAext (http://sirna.wi.mit.edu/), and then synthesized by BGI and cloned into a lentiviral pLKO.1 vector (cat. no. 10878; Addgene, Inc.). The sequences in *FOXO3a* and *SIRT6* targeted by the shRNAs were presented in Table II. Human full-length *SIRT6* (GenBank no. CR457200.1) cDNA was from MV3 cells via PCR; PrimeSTAR® Max DNA Polymerase (Takara Bio, Inc.) was used. Thermocycling conditions were as follows: 98˚C pre-denaturation for 5 min; then, 28 cycles of 98˚C for 30 sec, 60˚C for 30 sec and 72˚C for 20 sec; then, 72˚C for 10 sec. The products were constructed into a lentiviral pCDH-CMV-MCS-EF1-Puro vector (cat. no. CD510B; System Biosciences, LLC). The primers were listed in Table II. HA-FOXO3a WT plasmid (cat. no. 1787; Addgene, Inc.) was obtained from Addgene and then cloned into the pCDH-CMV-MCS-EF1-Puro vector. Plasmids were packaged into lentivirus as previously described (26). Briefly, 293FT cells (ATCC) were cultured in DMEM (Thermo Fisher Scientific, Inc.) with 10% FBS, 1% P/S and 0.5 mg/ml geneticin (Thermo Fisher Scientific, Inc.), which was replaced with lentiviral culture medium prior to transfection with plasmids, which was comprised of DMEM, 10% FBS, 2 mM L-glutamine (Invitrogen; Thermo Fisher Scientific, Inc.), 0.1 mM non-essential amino acid (Invitrogen; Thermo Fisher Scientific, Inc.) and 1 mM sodium pyruvate (Invitrogen; Thermo Fisher Scientific, Inc.). 293FT cells at 100% confluence were transfected with 0.625 μg of the plasmid of interest, plus the packaging plasmids pLP1, pLP2 and pLP/VSVG (Nova Lifetech, Inc.), using Opti-MEM™ medium (Gibco; Thermo Fisher Scientific, Inc.) and Lipofectamine™ 2000 (Thermo Fisher Scientific, Inc.). At 3 days later, the viral supernatant was aspirated with a syringe, filtered through a 0.45-μm filter membrane and collected in a 1.5-ml centrifuge tube. Fresh lentivirus culture medium was added to the 293FT cell culture wells, which were cultured for a further 48 h before collecting the second viral supernatant. Then, 40,000 MV3 cells in a 60-mm dish were infected with 2 ml lentivirus containing >10^7 TU/ml using 4 μg/ml polybrene (Sigma-Aldrich; Merck KGaA) and incubated at 37˚C with 5% CO_2 for 48 h. Then, the cells were re-seeded into a 100-mm petri dish and cultured in standard medium. After 3 days, 2 μg/ml puromycin was used to continuously screen the cells for ≥72 h. RT-qPCR or western blotting was performed to verify the expression of the target genes.

Western blot assay. Western blotting was conducted to analyze the expression of proteins. Briefly, cells at 80% confluence were trypsinized and collected in 5-ml tubes. Then, cells were centrifuged at 600 x g for 5 min at 4˚C, the supernatant was removed, and the cell pellet was washed three times with PBS. Protein was extracted from the cell pellet using RIPA lysis buffer (cat. no. P0013B; Beyotime Institute of Biotechnology), and the mixture was allowed to stand on ice for 30 min. The mixture was centrifuged at 12,000 x g at 4˚C for 15 min, and the protein concentration was determined by using an Enhanced BCA Protein Assay Kit (cat. no. P0009; Beyotime Institute of Biotechnology). Protein (100 μg/lane) was separated via 10% SDS-PAGE. Then, protein was transferred to PVDF membranes (cat. no. IPVH00010; Merck KGaA). Membranes were blocked with 5% BSA (Fraction V; cat. no. ST023; Beyotime Institute of Biotechnology) at room temperature for 2 h. Primary antibodies, including rabbit anti-FOXO3a

Table I. Primers used for reverse transcription-quantitative PCR.

Gene	Sequence (5'-3')
FOXO3A	F: ACGTCTTCAGGTCCTCCTGTT
	R: GGGGAAGCACCAAAGAAGAGAG
SIRT6	F: CTCGAAGTGGAGCTGGACC
	R: TCCTCGGGGATCATGGAGTC
GLUT1	F: TGTGTATGCCACCATTGGCT
	R: CTAGCGCGATGGTCATGAGT
GLUT4	F: GGACAGCCAGCCTACGCCACCATA
	R: GGACAGCCAGCCTACGCCACCATA
HK1	F: GCACGTTTGCACCATTGTCT
	R: TTGTGGAAACGCCGGGAATA
HK2	F: GAATGGGAAGTGGGGTGGAG
	R: GAGGAGGATGCTCTCGTCCA
HK3	F: TTCCCATGTAGGCAGCTTGG
	R: ATGAGGCCTATCTCGCAACG
GAPDH	F: CTCTGCTCCTCCTGTTCGAC
	R: GCGCCCAATACGACCAAATC
PFK1	F: CTGCCCCTCATGGAATGTGT
	R: ATACCGGGGGTCTGACATGA
PKM2	F: AATGCAGTCCTGGATGGAGC
	R: ACTGCAGCACTTGAAGGAGG
LDHA1	F: GGTCCTTGGGGAACATGGAG
	R: TAGCCCAGGATGTGTAGCCT
LDHA2	F: AGCTGTTCCACTTAAGGCCC
	R: AGGAATCGGGAATGCACGTC
ACTB	F: CGTCTTCCCCTCCATCGTG
	R: TCGATGGGGTACTTCAGGGT

F, forward; R, reverse; *FOXO3a*, forkhead box O3; *SIRT6*, sirtuin 6; *GLUT1/4*, glucose transporter 1/4; *HK1-3*, hexokinase 1-3; *PFK1*, phosphofructokinase 1; *PKM2*, pyruvate kinase isozyme M2; *LDHA1/2*, lactate dehydrogenase A1/A2; *ACTB*, β-actin.

Table II. Primers or targeted sequences for vector construction.

Primer/target site	Sequence (5'-3')
shFOXO3a#1	AATGTGACATGGAGTCCATTAT
shFOXO3a#2	GGACAATAGCAACAAGTATACC
shSIRT6	AAGAATGTGCCAAGTGTAAGA
Scramble	ATCCGTCCGAACGTAAGTCAA
SIRT6	Forward (*Eco*RI): CCGGAATTCAT GTCGGTGAATTACGCGGCGGC
	Reverse (*Bam*HI): CGCGGATCCTT AACTGGGGACCGCCTTGG

Underlined regions indicate recognition sites for the specified restriction enzyme. sh, short hairpin RNA; *SIRT6*, sirtuin 6; FOXO3a, forkhead box O3.

(1:1,000; cat. no. 2497; Cell Signaling Technology, Inc.), rabbit anti-SIRT6 (1:800; cat. no. 12486; Cell Signaling Technology, Inc.) and anti-α-Tubulin Antibody (1:200; cat. no. 2144; Cell Signaling Technology, Inc.) were incubated at 4˚C overnight. Then, horseradish peroxidase-conjugated goat anti-mouse (1:20,000; cat. no. ab205719; Abcam) or goat anti-rabbit IgG (1:20,000; cat. no. ab205718; Abcam) was incubated at room temperature for 2 h. ChemiSignal™ Plus ECL (Clinx Science Instruments Co., Ltd.) was used to visualize bands, which were imaged using a GenoSens 2000 Touch gel imaging system (Clinx Science Instruments Co., Ltd.).

MTT assay. Cells (1,000/well) were cultured in 96-well plates at 37˚C in a CO_2 incubator, and MTT assays were performed as previously described (27) at indicated times (0, 2, 4 and 6 days).

Glucose uptake assay. Cells ($2x10^5$/well) were cultured at 37˚C in a CO_2 incubator in glucose-free RPMI-1640 (Procell Life Science & Technology Co., Ltd.) with FBS and P/S in 6-well plates for 120 min, and the medium was removed. A fluorescent glucose analogue, 2-NBDG (100 μM), was dissolved in Kerbs-Ringer bicarbonate (KRB) buffer (129 mM NaCl, 4.8 mM KCl, 5 mM $NaHCO_3$, 1.2 mM $MgSO_4$, 2 mM $CaCl_2$ and 10 mM HEPES) and added to the plates prior to incubation at 37˚C for a further 120 min. The cells were collected using trypsin and washed with KRB buffer, and the fluorescence of 2-NBDG in the cells was detected via flow cytometry (Acurri C6; BD Biosciences) and analyzed by using FlowJo 7.6.1 (FlowJo LLC).

Glucose consumption, lactate and lactate dehydrogenase (LDH) assays. Cells ($2x10^5$/well) were cultured in 6-well plates at 37˚C for 48 h. The glucose content in the medium was detected using a Glucose Assay kit (cat. no. GAGO20; Sigma-Aldrich; Merck KGaA), the lactate content in the medium was detected using a Lactate Assay kit (cat. no. MAK064; Sigma-Aldrich; Merck KGaA) and the lactate dehydrogenase activity of cells was detected using a lactate dehydrogenase assay kit (cat. no. MAK066; Sigma-Aldrich; Merck KGaA), all according to the manufacturer's protocols. Samples were analyzed using a SYNERGY HTX multi-mode reader (Biotek Instruments, Inc.). The rates of glucose consumption, lactate production and relative LDH activity were calculated according to the standard curve line and OD value of each sample. Then, these values were also normalized by cell numbers determined by using a blood cell counting chamber.

Glucose stress flux test. A glucose stress flux test was conducted as previously reported (14). In brief, 40,000 cells were seeded into XF96 cell culture microplates and cultured at 37˚C for 24 h. The medium was then replaced with Seahorse XF DMEM (Agilent Technologies, Inc.) containing 2 μM glutamine, and the microplates were maintained in a non-CO_2 incubator at 37˚C for 60 min. Then, a Seahorse XF glycolytic stress test was performed using a Seahorse XFp analyzer (Agilent Technologies, Inc.). In this test, a final concentration of 10 μM glucose (Sangon Biotech Co., Ltd.), 1 μg/ml oligomycin (cat. no. 495455; Sigma-Aldrich; Merck

KGaA) and 50 μM 2-deoxyglucose (Sangon Biotech Co., Ltd.) were used.

Chromatin immunoprecipitation (ChIP) assay. ChIP assays were performed in MV3 cells by using the EZ CHIP™ kit (cat. no. 17-371; Merck KGaA) according to the manufacturer's protocol. 293FT cells were cultivated in a 100-mm dish; when the cells reached 80% confluence, 1% fresh formaldehyde (Sangon Biotech Co., Ltd.) was added and the cells were cultured in a 37˚C incubator for 10 min to crosslink protein and DNA. The cells were washed with PBS buffer containing 1 mM phenylmethylsulfonylfluoride (PMSF; cat. no. ST505; Beyotime Institute of Biotechnology), and then collected in a 1.5-ml tube for centrifugation at 1,000 x g for 2 min at 4˚C. The centrifuged cell pellet was resuspended in 200 μl SDS lysis buffer (cat. no. P0013G; Beyotime Institute of Biotechnology) containing 1 mM PMSF on ice for 10 min, following which it was subjected to ultrasonic vibration with 15 sec ON, 30 sec OFF for 8 cycles on ice to break the genomic DNA into <1,000-bp fragments. The sample was then resuspended in sodium chloride, incubated at 65˚C for 4 h, and then mixed with Tris-balanced phenol and centrifuged at 12,000 x g at 4˚C for 5 min. Finally, 200 μl chloroform was added to the pellet, which was then centrifugated at 4˚C at 12,000 x g for 5 min.

The resulting supernatant was moved into an ice-cold centrifuge tube, and ChIP dilution buffer containing 1 mM PMSF was added to a final volume of 2 ml, of which 20 μl was collected to use as the input control. Then, 70 μl of Protein A + G Agarose (containing salmon sperm DNA) was added to the remaining sample, which was incubated slowly at 4˚C on a shaker for 30 min. The solution was then centrifuged at 1,000 x g for 1 min at 4˚C. and the supernatant was collected. Then, 2 μg FOXO3a primary antibody (cat. no. ab12162; Abcam) or rabbit IgG (cat. no. A7016, Beyotime Institute of Biotechnology) as a blank control was added, along with 60 μl Protein A + G Agarose containing salmon sperm DNA; the mixture was incubated slowly at 4˚C on a shaker for 60 min and subsequently centrifuged at 1,000 x g for 1 min at 4˚C. The supernatant was removed, and the pellet was centrifuged once at 1,000 x g for 1 min at 4˚C with 1 ml Low Salt Immune Complex Wash Buffer, High Salt Immune Complex Wash Buffer and LiCl Immune Complex Wash Buffer, followed by centrifugation under the same conditions with 1 ml TE Buffer twice. Elution Buffer was subsequently added prior to centrifugation at 1,000 x g for 1 min at 4˚C, following which this step was repeated. The resulting supernatant was collected, the sample was recovered and concentrated using a AxyPrep DNA Gel Extraction kit (Axygen Bioscience, Inc.), and then subjected to qPCR analysis using the primers in Table III.

Dual-luciferase assay and promoter analysis. To analyze the similarity of the promotor region of human and mouse *SIRT6*, the promoter region (-2,500 to 0 bp) of mouse *SIRT6* and the promoter region (-2,500 to 0 bp) of human *SIRT6* were compared using the online Bl2seq tool in the SilkDB (http://www.silkdb.org/silkdb/). The sequences in the promoter regions, which were termed 0.1 k (-1,100 to -939 bp), 0.2 k (-1,147 to -939 bp), 0.6 k (-1,538 to -939 bp), 1.2 k (-2,152 to -939 bp) and N0.9 k (-938 to -25 bp), were obtained from genomic DNA extracted from MV3 cells via PCR by using primers in Table III. The mutant (Mut) sequence of SIRT6 promoter region was synthesized by Sangon Biotech Co., Ltd. These sequences were cloned into pGL3-basic luciferase reporter vectors (cat. no. E1751; Promega Corporation). Then, 1 μg pGL3 vector and 1 μg pRL-TK expressing *Renilla* luciferase (Youbio, Inc.) were co-transfected into 20,000 MV3 cells/well in a 24-well plate with X-tremeGENE™ HP DNA Transfection reagent (cat. no. 6366546001; Roche Diagnostics), and the luciferase assay was performed as previously described using a Dual-Lumi™ Luciferase Reporter Gene assay kit (cat. no. RG088S; Beyotime Institute of Biotechnology) (28). The promotor activity was normalized to *Renilla* luciferase activity.

The profile of FOXO3a in *Mus musculus* and *Homo sapiens* was downloaded from the JASPER database (version 5.0_ALPHA; http://jaspar.binf.ku.dk/) and then compared with the promoter region of human *SIRT6* to find the potential binding site of FOXO3a.

Tumor xenografts. The animal experiments in the current study were approved and supervised by the Institutional Animal Care and Use Committees of the Southwest University (permit no. IACUC-20190402-02) and the Experimental Animal Care and Use Committees of the Institute of Sericulture and Systems Biology. The study was performed according to the Laboratory Animal Management Regulations and the Measures of Chongqing Municipality on the Management of Experimental Animals. A total of nine 4-week-old female mice (weight, 18-20 g; BALB/c-nu; Beijing Huafukang Bioscience Co. Ltd.) were purchased and housed in a specific pathogen-free room to acclimate for ~1 week. The animals were house at 22˚C with 40-60% humidity under a 12:12-h light/dark cycle. Mice were provided *ad libitum* access to food and water. Then, MV3 cells ($1x10^6$) in 100 μl PBS were subcutaneously injected into the left flank of mice. Every group contained ≥3 mice. Then, 10 days later, the first measurements of the length and width of tumors were made by caliper, and tumor growth was measured for 25 days after this point. The tumor volume was calculated with the following formula: Volume = tumor length x width^2 x π/6. At the end of the experiment, animals was sacrificed with CO_2 in a 10-l volume chamber with a flow rate of 2 l/min and a displacement rate of 20% volume/min, and then tumors were removed and weighed. The maximum tumor diameter observed was 1.37 cm.

Bioinformatics analysis. The Cancer Genome Atlas (TCGA) Ocular melanoma (project no. TCGA-UVM) dataset was downloaded from University of California Santa Cruz Xena (http://xena.ucsc.edu/). Other clinical databases, including Tumor Melanoma Metastatic Bhardwaj-44-MAS5.0-u133p2, Mixed Melanoma Briggs-70-MAS5.0-u133a, Mixed Melanoma (Metastasis) Hynes-83-MAS5.0-u133a, Exp Cellline Melanoma-Exosome McMasters-8-MAS5.0-u133p2, Exp Melanoma Augustine-50-MAS5.0-u133p2, Tumor Melanoma Jönsson-214-custom-ilmnht12v4 and Tumor Melanoma (Metastatic) Matta-87-MAS5.0-u133p2 were downloaded from the public R2 platform (https://hgserver1.amc.nl/). Genes in certain datasets were further analyzed by using alternative probes provided by the databases. All data were analyzed by using the software GraphPad Prism 6 (GraphPad Software, Inc.).

Table III. *SIRT6* primers used for chromatin immunoprecipitation and luciferase assays.

Primer	Sequence (5'-3')
SIRT6-p	F1: AAGACAATCCGTGGGCTTGG
	R1: GAGCTACCCAGGTACCCTG
	F2: TGGCTAGGACTCAGCACG
	R2: TAGGGGAGGAAGGAGGTGG
SIRT6-p-0.1k	F (*Nhe*I): CCGGCTAGCGCCCGGCTCACTCACTTTTTAG
SIRT6-p-0.2k	F (*Nhe*I): CCGGCTAGCCTGCCTTGGCCTCCCAAAGT
SIRT6-p-0.6k	F (*Nhe*I): CCGGCTAGCCTATCATCACTGGACTGATTTCAGTTTC
SIRT6-p-1.2k	F (*Nhe*I): CCGGCTAGCGGGTAATAAGACACCCAACAGAGG
SIRT6-p- (all)	R (*Xho*I): CCGCTCGAGGTAATGGTGACATGGTGTGGTTG
SIRT6-p-N0.9k	F (*Nhe*I): CCGGCTAGCCTGGTCACATGTTTGTGTCCAC
SIRT6-p-N0.9k	R (*Xho*I): CCGCTCGAGAAAGTTTCCCTTGTTGAGGCCG

Underlined regions indicate recognition sites for the specified restriction enzyme. *SIRT6*, sirtuin 6; F, forward; R, reverse.

Statistical analysis. All the experiments were repeated 3 times and the data collected were analyzed by using GraphPad Prism 6. Data were presented as the mean ± SD. Unpaired two-tailed Student's t-test was applied to determine significant differences between two groups. The scan cutoff modus was used to separate high- and low-expression groups for Kaplan-Meier analysis, with the exception of the analysis of data from the Cancer Genome Atlas (TCGA) Ocular melanoma (project no. TCGA-UVM) dataset, for which the median cutoff modus was used. Log-rank (Mentel-Cox) tests were conducted to determine significance for survival analysis. A Bonferroni correction was applied after the log-rank test to control for multiple comparisons [$P<0.00833$ (0.05/6) was considered to indicate a statistically significant different for this analysis]. Pearson correlation coefficient was used to analyze the correlation of the expression levels of 2 genes. One-way ANOVA followed by Dunnett's test was performed to compare the mean of each experiment group with the control group in datasets containing multiple comparisons. One-way ANOVA followed by Tukey's test was performed to compare the mean of each group with the mean of every other group when performing multiple comparisons. $P<0.05$ was considered to indicate a statistically significant difference.

Results

High FOXO3A expression predicts improved prognosis of patients with melanoma. To elucidate the relationship between *FOXO3A* mRNA expression and the prognosis of patients with melanoma, its expression was analyzed in the database termed Tumor Melanoma Metastatic Bhardwaj-44-MAS5.0-u133p2 from the R2 platform. The results showed that high *FOXO3A* expression predicted improved overall survival and metastasis-free survival in this cohort (Fig. 1A and B). Furthermore, *FOXO3A* expression was negatively associated with the survival rate of patients with metastatic melanoma (Figs. 1C and S1A-D). Additionally, *FOXO3A* expression was lower in patients with stage IV melanoma than those with stage III melanoma (Figs. 1D, and S1E and F). Importantly, *FOXO3A* expression was lower in nevus compared to normal tissues, and *FOXO3A* expression was further decreased in melanoma compared with nevus (Fig. 1E). Next, in the database termed Mixed Melanoma (Metastasis) Hynes-83-MAS5.0-u133a, it was found that *FOXO3A* expression was lower in melanoma metastasis compared with the primary tumors (Fig. 1F). In an experimental database termed Exp Cellline Melanoma-Exosome McMasters-8-MAS5.0-u133p2, it was demonstrated that *FOXO3A* expression was lower in the exosomes of A375 melanoma cells compared to those of HeMa-LP normal melanocytes (Fig. 1G). N-Ras mutations arise in 15-20% of all melanomas, and have been shown to be associated with aggressive clinical behavior and poor prognosis (29). Of note, *FOXO3A* expression was lower in N-Ras mutant melanoma cells compared with wild-type cells (Fig. 1H). These results implied that FOXO3a may act as a tumor suppressor in melanoma.

FOXO3A transcriptionally promotes the expression of SIRT6 in melanoma. It was previously shown that the FOXO3a genotype was strongly associated with human longevity (30). As a deacetylase, SIRT6 also was shown to be related to human longevity (31). Additionally, FOXO3a and SIRT6 are both regulators of hepatic sterol regulatory element-binding protein 2 and cholesterol biosynthesis, as well as low-density lipoprotein-cholesterol homeostasis (32,33). These findings suggested that FOXO3a and SIRT6 are highly associated; however, their relationship had not been elucidated. In the present study, it was found that *FOXO3A* mRNA expression was positively correlated with *SIRT6* mRNA expression (detected by probe 219613_s_at or 233179_x_at) in a melanoma cohort (Fig. 2A and B). Additionally, mRNA expression levels of *FOXO3A* and *SIRT6* were correlated with each other in PIG1 melanocytes and 3 melanoma cell lines (Fig. 2C-E). Furthermore, FOXO3a expression was silenced in MV3 melanoma cells via virus-mediated transfection, and the results showed that both the mRNA and protein levels of SIRT6 were downregulated after FOXO3a silencing (Fig. 2F and G). Consistently, FOXO3a overexpression also induced upregulation of SIRT6 expression in MV3 cells (Fig. 2H and I).

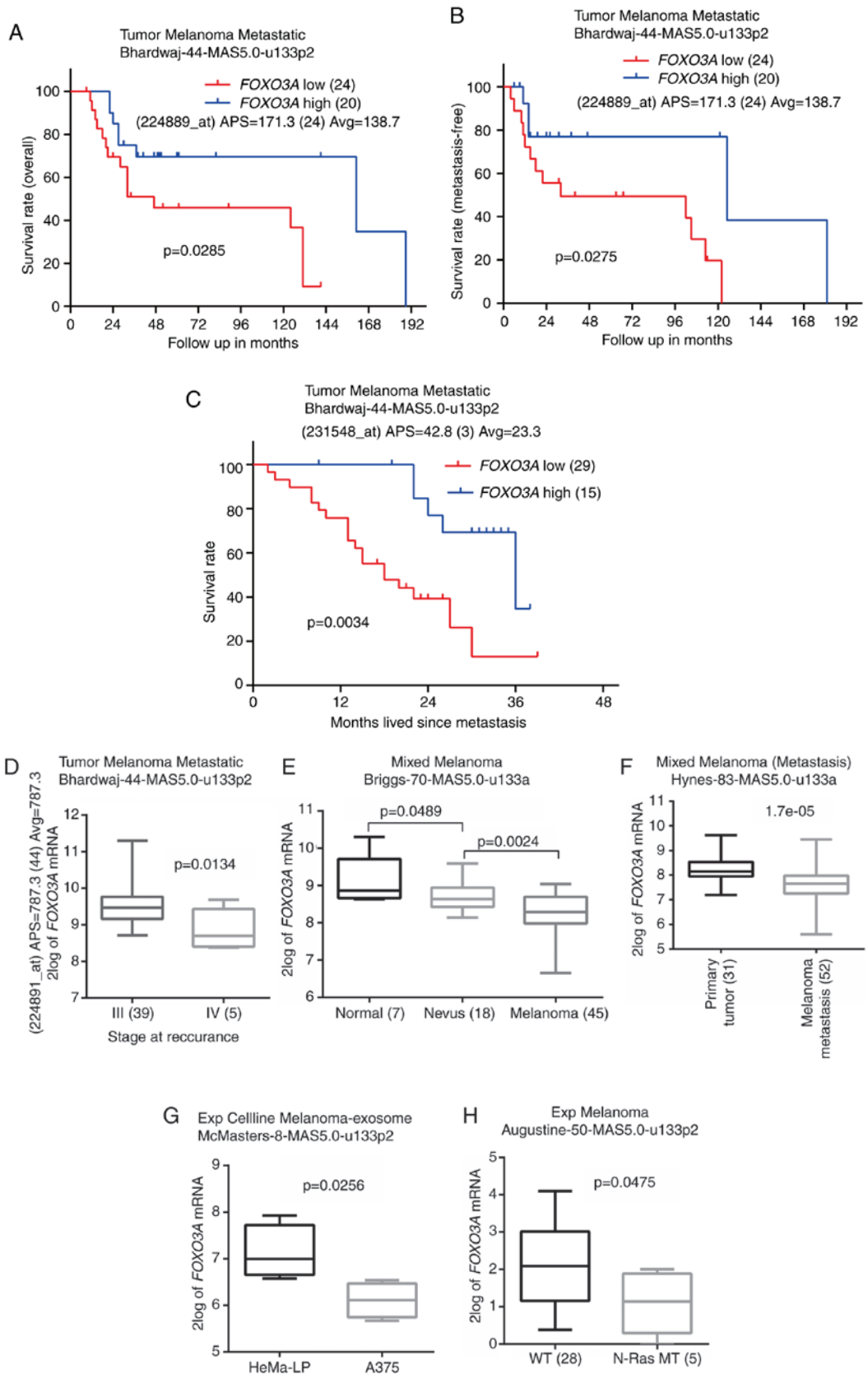

Figure 1. High *FOXO3A* expression predicts improved prognosis for patients with melanoma. (A and B) Relationship between *FOXO3A* expression, and overall and metastasis-free survival in the database termed Tumor Melanoma Metastatic Bhardwaj-44-MAS5.0-u133p2 from the R2 platform. (C) Relationship between *FOXO3A* expression and the survival rate following metastasis in the database termed Tumor Melanoma Metastatic Bhardwaj-44-MAS5.0-u133p2. (D) Expression of *FOXO3A* in stage III and IV melanoma in the Tumor Melanoma Metastatic Bhardwaj-44-MAS5.0-u133p2 database. (E) Expression of *FOXO3A* in normal tissues, nevus and melanoma in the database termed Mixed Melanoma Briggs-70-MAS5.0-u133a. (F) Expression of *FOXO3A* in primary melanoma and melanoma metastases in Mixed Melanoma (Metastasis) Hynes-83-MAS5.0-u133a database. (G) Expression of *FOXO3A* in the exosomes of MeLa-LP normal melanocytes and A375 melanoma cells in the database termed Exp Cellline Melanoma-Exosome McMasters-8-MAS5.0-u133p2. (H) Expression of *FOXO3A* in WT melanoma cells and N-Ras MT melanoma cells in the database termed Exp Melanoma Augustine-50-MAS5.0-u133p2. *FOXO3A*, forkhead box O3; WT, wild-type; MT, mutant.

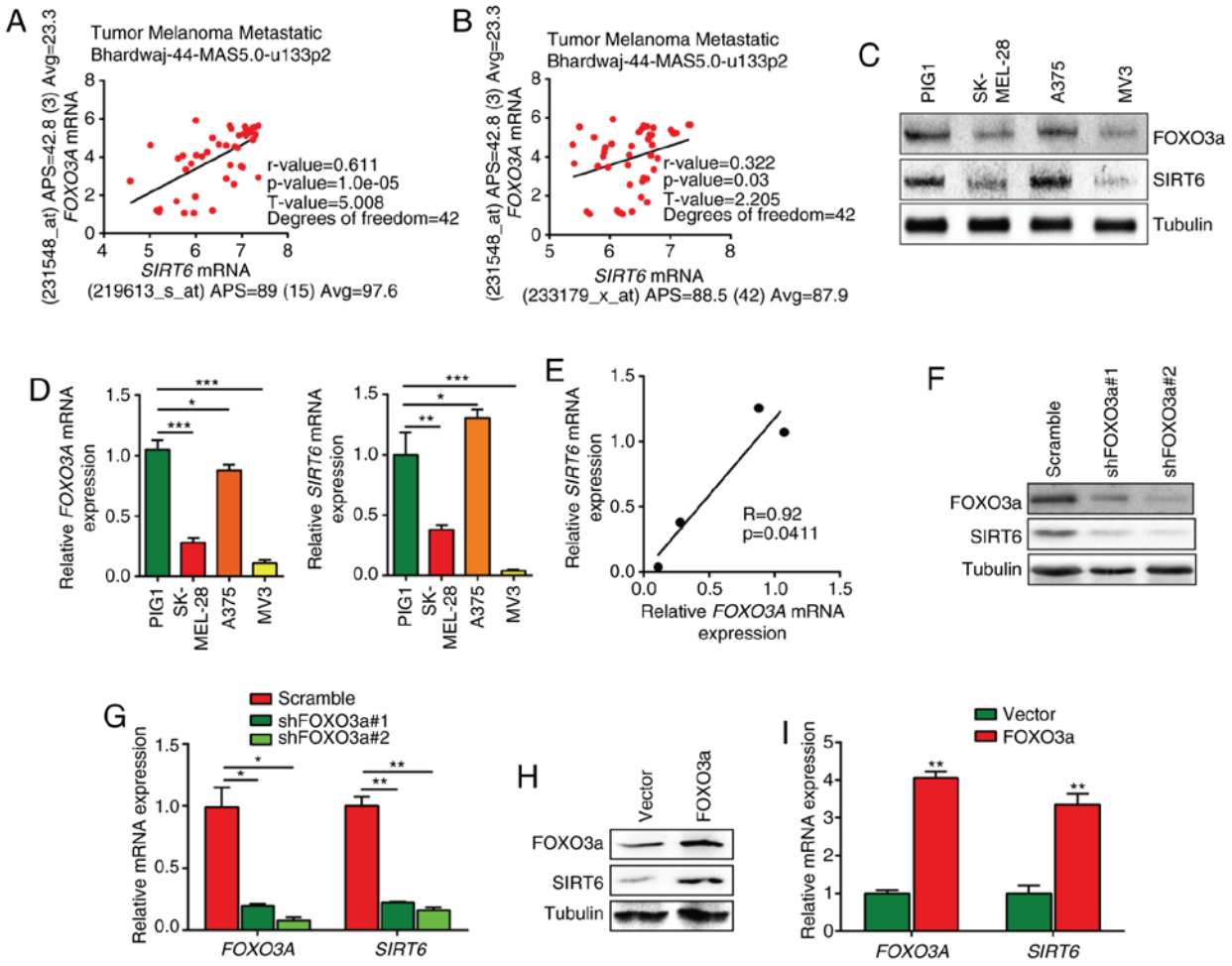

Figure 2. FOXO3a transcriptionally regulates the expression of *SIRT6* in melanoma. (A and B) Correlation of *FOXO3A* expression and *SIRT6* expression in a melanoma cohort detected using different *SIRT6* probes. (C) Western blotting was performed to detect the protein expression of FOXO3a and SIRT6 in PIG1 normal melanocytes and 3 different melanoma cell lines. (D) RT-qPCR was used to detect the mRNA expression of *FOXO3A* and *SIRT6* in 4 different cell lines. One-way ANOVA followed by Dunnett's test was performed to compare the mean of melanoma cell group with PIG1 melanocytes. *P<0.05, **P<0.01, ***P<0.001 vs. PIG1. (E) Correlation of *FOXO3A* mRNA expression and SIRT6 expression in 4 different cell lines. (F) Expression of FOXO3a and SIRT6 as detected via western blotting in MV3 cells after FOXO3a silencing. (G) Relative expression of *FOXO3A* and *SIRT6* detected via RT-qPCR in MV3 cells after FOXO3a silencing. *P<0.05, **P<0.01 vs. Scramble. (H) Expression of FOXO3a and SIRT6 detected via western blotting in MV3 cells after FOXO3a overexpression. (I) Relative expression of *FOXO3A* and *SIRT6* detected via RT-qPCR in MV3 cells after FOXO3a overexpression. **P<0.01 vs. Vector.

A previous study reported that FOXO3a regulated the transcription of *SIRT6* by binding and activating nuclear respiratory factor 1 (NRF1) in the mouse (34). However, the promoter of human *SIRT6* was not similar with the promoter in mouse *SIRT6*. No NRF1-binding sites (5'AGGGCGCATGCGCCC TC3') were identified in the promoter regions (-2,500 to 0 bp) of human *SIRT6*, implying that FOXO3a may regulate the transcription of *SIRT6* through another mode of action (data not shown). The promoter region (-2,500 to 0 bp) of mouse *SIRT6* and the promoter region (-2,500 to 0 bp) of human *SIRT6* were analyzed by using the online Bl2seq tool in the SilkDB. The results showed that there were several similar DNA sequences in both promoters (Fig. 2J). It was hypothesized that the binding sites of FOXO3a in the promoter region of SIRT6 may be conserved in mammals. Therefore, these DNA sequences may be candidate binding sites. Therefore, several regions (0.1, 0.2, 0.6, 1.2 and N0.9 k) were cloned from the promoter of human *SIRT6* and constructed into pGL3 vectors (Fig. 2J). A dual-luciferase assay showed that only the -2,128 to -1,514 bp region exhibited significant activity compared with other regions (Fig. 2J). As there were four candidate binding sites for FOXO3a in this region, ChIP RT-qPCR assays were used to detect the precise binding site. The results showed that FOXO3a exhibited significant enrichment in the -2,083 to -1,859 bp region, with no enrichment in the -1,852 to -1,746 bp region (Fig. 2K and L). Then, the -2,083 to -1,859 bp region was analyzed in the JASPER website. The profile of FOXO3a in *Mus musculus* and *Homo sapiens* (Fig. 2M) was used to find the specific binding site in the -2,083 to -1,859 bp region of the *SIRT6* promoter. It was shown that there was a predicted site sequence (5'GGTAAATA3') that was highly similar to the FOXO3a binding profile (Fig. 2N). Then, wild-type (WT) and Mut sequences of this region were synthesized and cloned into a pGL3 vector (Fig. 2N). A luciferase activity assay revealed that -2,083 to -1,859 WT showed a similar level of promoter activity as the -2,128 to -914 bp region, whereas -2,083 to -1,859 Mut significantly decreased promoter activity (Fig. 2O). These results indicated that FOXO3a regulated *SIRT6* expression in human melanoma cells via a transcriptional manner that is distinct from that in the mouse.

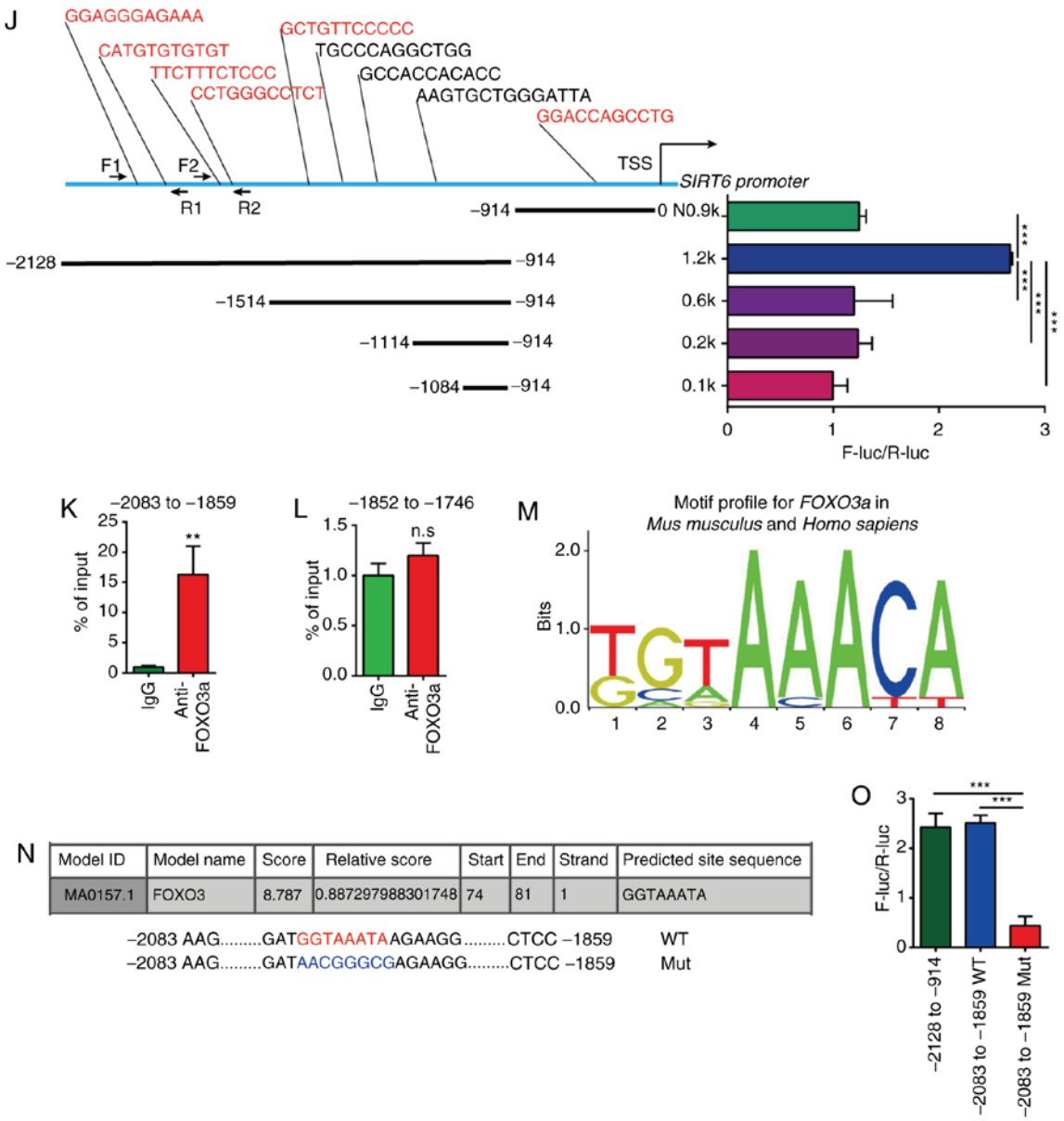

N

Model ID	Model name	Score	Relative score	Start	End	Strand	Predicted site sequence
MA0157.1	FOXO3	8.787	0.887297988301748	74	81	1	GGTAAATA

−2083 AAG.....GATGGTAAATAAGAAGG.....CTCC −1859 WT
−2083 AAG.....GATAACGGGCGAGAAGG.....CTCC −1859 Mut

Figure 2. Continued. (J) Overview of insert fragments in pGL3 vectors used in dual-luciferase assays and ChIP primers designed based on the promoter of the human *SIRT6* gene. Firefly luciferase/Renilla luciferase (F-luc/R-luc) was shown. *SIRT6* promoter (different regions) activity was detected by dual-luciferase assays in MV3 cells. One-way ANOVA followed by Tukey's test was performed to compare groups. ***P<0.001. (K and L) CHIP RT-qPCR assay was used to detect the enrichment of FOXO3a in the promoter region of *SIRT6* in MV3 cells. **P<0.01 vs. IgG. n.s., not significant. (M) Logo for FOXO3a in *Mus musculus* and *Homo sapiens* was downloaded from the JASPER website. (N) Prediction of FOXO3a binding site in the -2,083 to -1,859 bp region of the *SIRT6* promoter. Then, WT and Mut versions of this sequence were inserted into luciferase vectors. (O) *SIRT6* promoter (-2,128 to -914, -2,083 to -1,859 WT and -2,083 to -1,859 Mut) activity was detected by dual-luciferase assay in MV3 cells. ***P<0.001 vs. -2128 to -914. FOXO3a, forkhead box O3; SIRT6, sirtuin 6; RT-qPCR, reverse transcription-quantitative PCR; ChIP, chromatin immunoprecipitation; F-luc, firefly luciferase; R-luc, *Renilla* luciferase; sh, short hairpin (RNA); WT, wild-type; Mut, mutant

FOXO3a is negatively correlated with aerobic glycolytic genes in melanoma cohorts. SIRT6 is a major regulator of aerobic glycolysis (26), which is an important cause of tumor progression. Whether FOXO3a also contributed to the aerobic glycolysis in melanoma was explored. By analyzing data from clinical databases, the results showed that *FOXO3A* mRNA expression was negatively correlated with the expression of a cluster of genes that participate in aerobic glycolysis, such as hexokinase 1 (*HK1*), HK3, phosphofructokinase (*PFK*) muscle, PFK fructobiphosphatase 3, pyruvate kinase isozyme (*PKM*) and *LDHA* (Figs. 3A-F and S2A-O). Notably, the majority of these genes are also targets of SIRT6 (35). These results implied that FOXO3a-SIRT6 may be a major regulator controlling the expression of these glycolytic genes in melanoma.

SIRT6 overexpression rescues FOXO3a deficiency-induced upregulation of aerobic glycolysis. To validate the hypothesis that FOXO3a-SIRT may regulate glycolysis in melanoma cells, SIRT6 was overexpressed using a SIRT6 overexpression vector (Fig. 4A and B) in FOXO3a-silenced MV3 cells (Fig. 4C and D). The results revealed that FOXO3a silencing induced upregulation of a cluster of glycolytic genes, including glucose transporter 4 (*GLUT4*), *GLUT1, HK1, HK2, HK3, GAPDH, PFK1, PKM2*, lactate dehydrogenase A1 (*LDHA1*) and *LDHA2* (Fig. 4D). However, this effect was rescued by

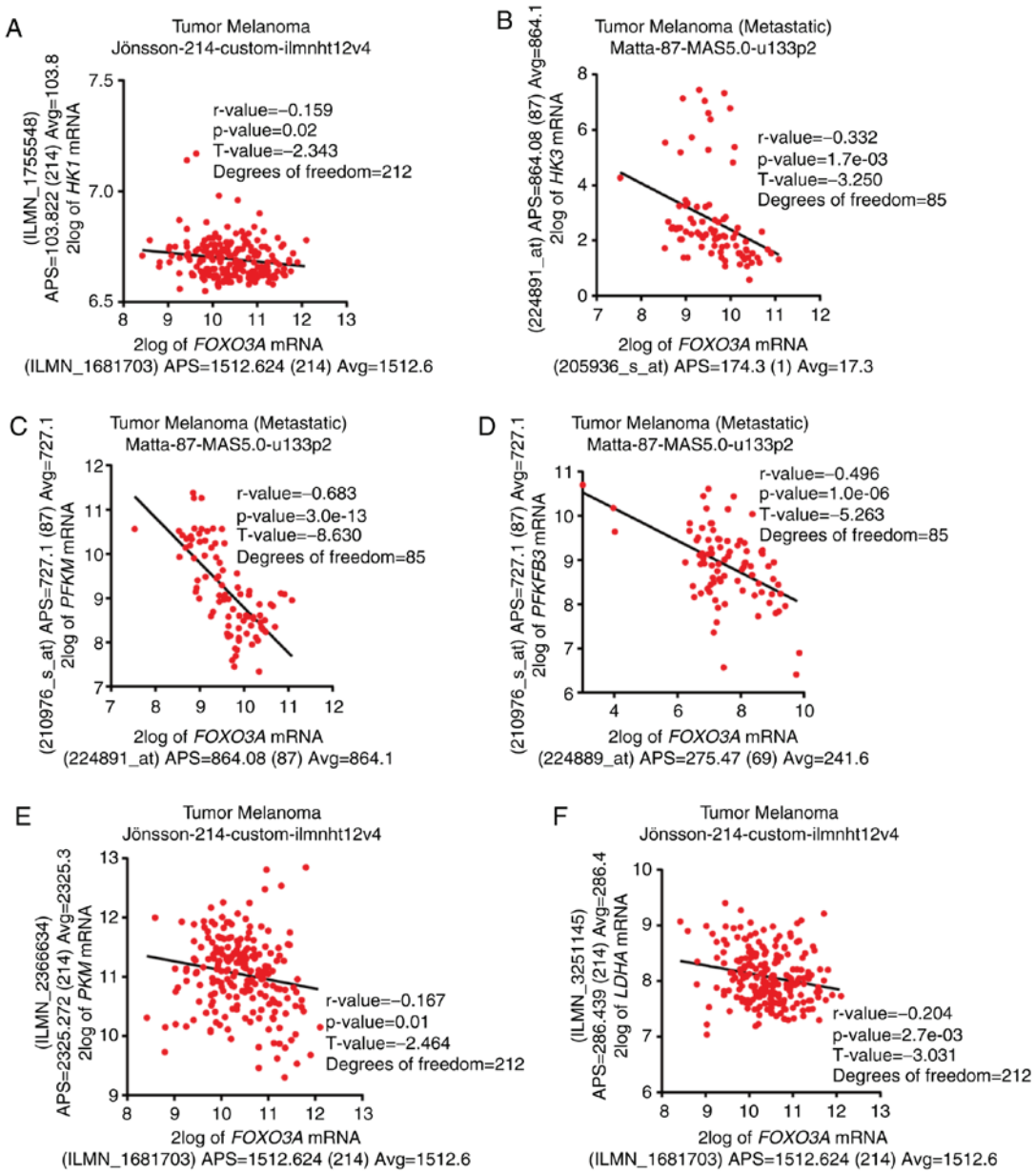

Figure 3. *FOXO3a* is negatively correlated with aerobic glycolysis-associated genes in melanoma cohorts. Correlation of *FOXO3A* expression and the expression of glycolysis genes, including (A) *HK1*, (B) *HK3*, (C) *PFKM*, (D) *PFKFB3*, (E) *PKM* and (F) *LDHA* in melanoma cohorts. *HK*, hexokinase; *PFK*, phosphofructokinase; *PFKM*, PFK muscle; *PFKFB3*, PFK fructobiphosphatase 3; *PKM*, pyruvate kinase isozyme; *LDHA*, lactate dehydrogenase A.

overexpression of SIRT6 (Fig. 4D). Additionally, FOXO3a silencing markedly promoted glucose uptake in MV3 cells (Fig. 4E). Consistently, FOXO3a-induced glucose uptake was also recovered by SIRT6 overexpression (Fig. 4E). Then, the glucose consumption, lactate production and LDH activity of MV3 cells were detected. The results showed that FOXO3a silencing upregulated aerobic glycolysis, whereas SIRT6 overexpression rescued this effect (Fig. 4F-H). The glycolytic flux test was performed using a Seahorse XFp analyzer in FOXO3a-silenced MV3 cells after SIRT6 restoration, with the results showing that glycolytic flux was notably increased after FOXO3a silencing, whereas SIRT6 overexpression returned glycolytic flux to the levels of the control group (Fig. 4I). These results indicated that the FOXO3a-SIRT6 axis serves an important role in controlling the aerobic glycolysis of melanoma cells.

SIRT6 downregulation retrieves FOXO3a overexpression-induced decrease of aerobic glycolysis. To further validate these results, SIRT6 was knocked down using a SIRT6 shRNA (Fig. 5A and B) in FOXO3a-overexpressing MV3 cells (Fig 5C and D). The results showed that SIRT6 silencing rescued the FOXO3a overexpression-induced downregulation of glycolytic genes, decrease in glucose uptake, decline in glucose consumption, reduction of lactate production, attenuation of LDH activity and upregulation of glycolytic flux (Fig. 5E-I). These results further indicated that the FOXO3a-SIRT6 axis was a major regulator of cellular metabolism in melanoma cells.

FOXO3a-SIRT6 axis contributes to melanoma cell viability in vitro and tumorigenicity in vivo. The effect of this regulatory axis on the viability of melanoma cells was subsequently

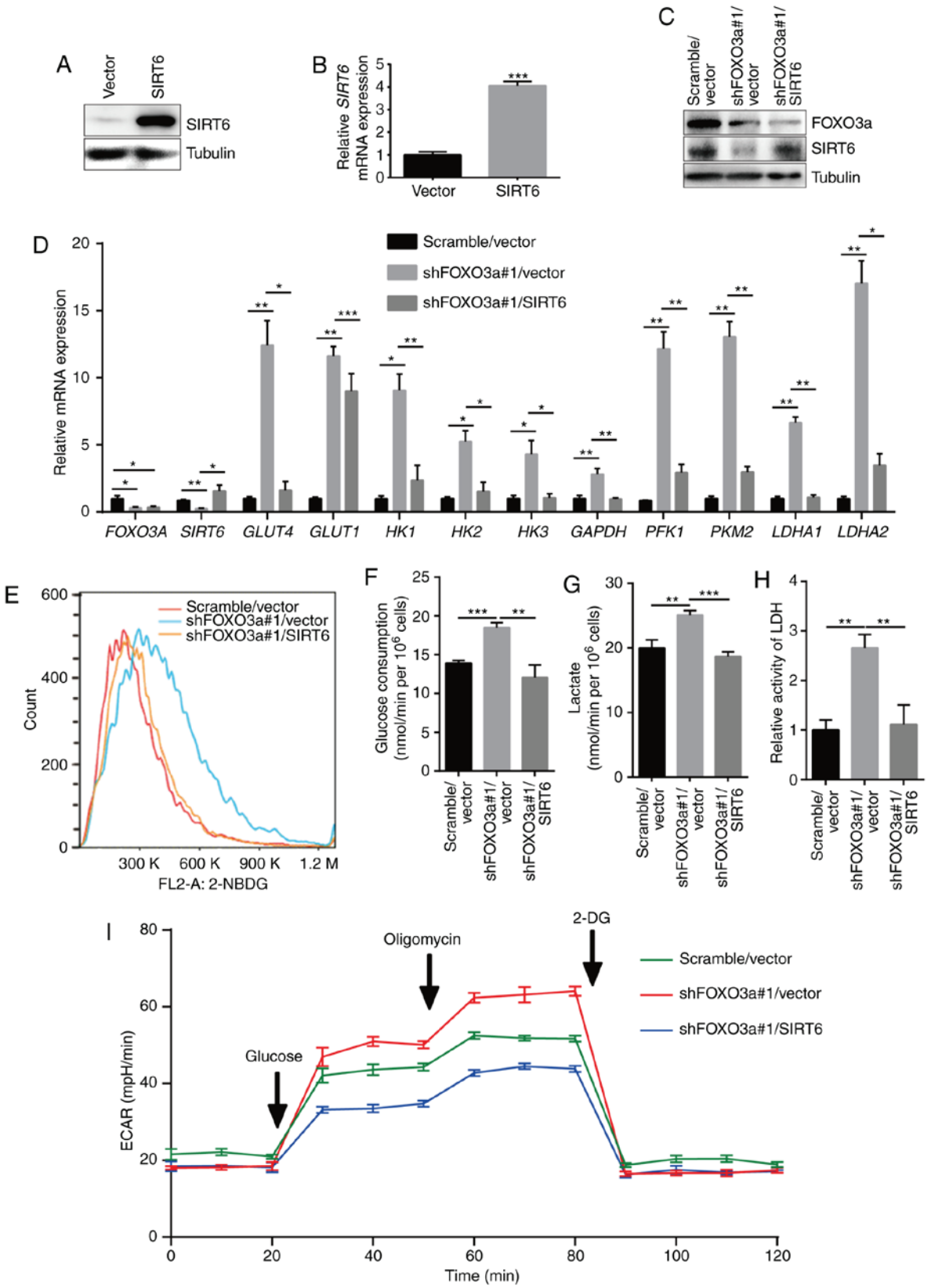

Figure 4. SIRT6 overexpression rescues FOXO3a deficiency-induced upregulation of aerobic glycolysis. SIRT6 overexpression was confirmed via (A) western blot and (B) RT-qPCR analyses in MV3 cells infected with SIRT6 overexpression vector. (C) Western blotting was used to detect the protein expression of FOXO3a and SIRT6 in FOXO3a-silenced MV3 cells after SIRT6 restoration. (D) Relative expression of SIRT6 target glycolysis-associated genes as determined via RT-qPCR in FOXO3a-silenced MV3 cells following SIRT6 restoration. (E) Glucose uptake detected by flow cytometry in FOXO3a-silenced MV3 cells after SIRT6 restoration. (F) Glucose consumption detected in FOXO3a-silenced MV3 cells after SIRT6 restoration. (G) Lactate production detected using a lactate assay kit in FOXO3a-silenced MV3 cells after SIRT6 restoration. (H) LDH activity detected using an LDH assay kit in FOXO3a-silenced MV3 cells after SIRT6 restoration. (I) Glycolytic stress flux test was conducted by using a Seahorse XF analyzer in FOXO3a-silenced MV3 cells after SIRT6 restoration. *P<0.05, **P<0.01, ***P<0.001. FOXO3a, forkhead box O3; SIRT6, sirtuin 6; RT-qPCR, reverse transcription-quantitative PCR; *HK*, hexokinase; *GLUT*, glucose transporter; *PFK1*, phosphofructokinase 1; *PKM2*, pyruvate kinase isozyme 2; *LDHA*, lactate dehydrogenase A; LDH, lactate dehydrogenase; sh, short hairpin (RNA); 2-NBDG, 2-Deoxy-2-[(7-nitro-2,1,3-benzoxadiazol-4-yl)amino]-D-glucose; ECAR, extracellular acidification rate; 2-DG, 2-deoxy-D-glucose.

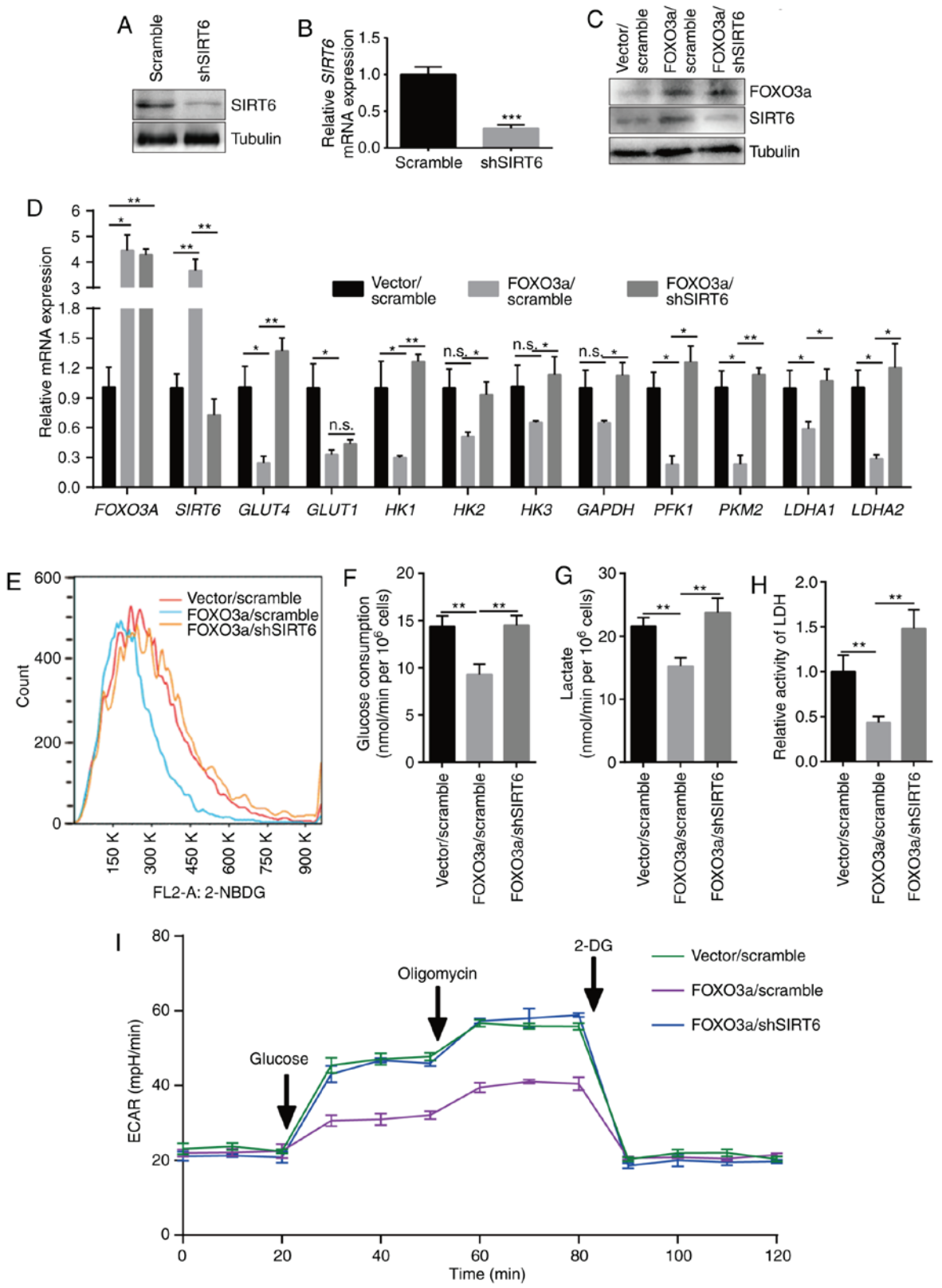

Figure 5. SIRT6 downregulation rescues FOXO3a overexpression-induced downregulation of aerobic glycolysis. SIRT6 knockdown was confirmed via (A) western blotting and (B) RT-qPCR in MV3 cells infected with shSIRT6. (C) Western blotting was used to detect the protein expression of FOXO3a and SIRT6 in FOXO3a-overexpressing MV3 cells after SIRT6 silencing. (D) Relative expression of SIRT6 target glycolysis-associated genes detected by RT-qPCR in FOXO3a-overexpressing MV3 cells after SIRT6 silencing. (E) Glucose uptake detected by flow cytometry in the 2-NBDG-treated FOXO3a-overexpressing MV3 cells after SIRT6 silencing. (F) Glucose consumption detected in FOXO3a-overexpressing MV3 cells after SIRT6 silencing. (G) Lactate production detected using a lactate assay kit in FOXO3a-overexpressing MV3 cells after SIRT6 silencing. (H) LDH activity detected using an LDH assay kit in FOXO3a-overexpressing MV3 cells after SIRT6 silencing. (I) Glycolytic stress flux test was conducted by using a Seahorse XF analyzer in FOXO3a-overexpressing MV3 cells after SIRT6 silencing. *P<0.05, **P<0.01, ***P<0.001. n.s., not significant. FOXO3a, forkhead box O3; SIRT6, sirtuin 6; RT-qPCR, reverse transcription-quantitative PCR; *HK*, hexokinase; *GLUT*, glucose transporter; *PFK1*, phosphofructokinase 1; *PKM2*, pyruvate kinase isozyme 2; *LDHA*, lactate dehydrogenase A; LDH, lactate dehydrogenase; sh, short hairpin (RNA); 2-NBDG, 2-Deoxy-2-[(7-nitro-2,1,3-benzoxadiazol-4-yl) amino]-D-glucose; ECAR, extracellular acidification rate; 2-DG, 2-deoxy-D-glucose.

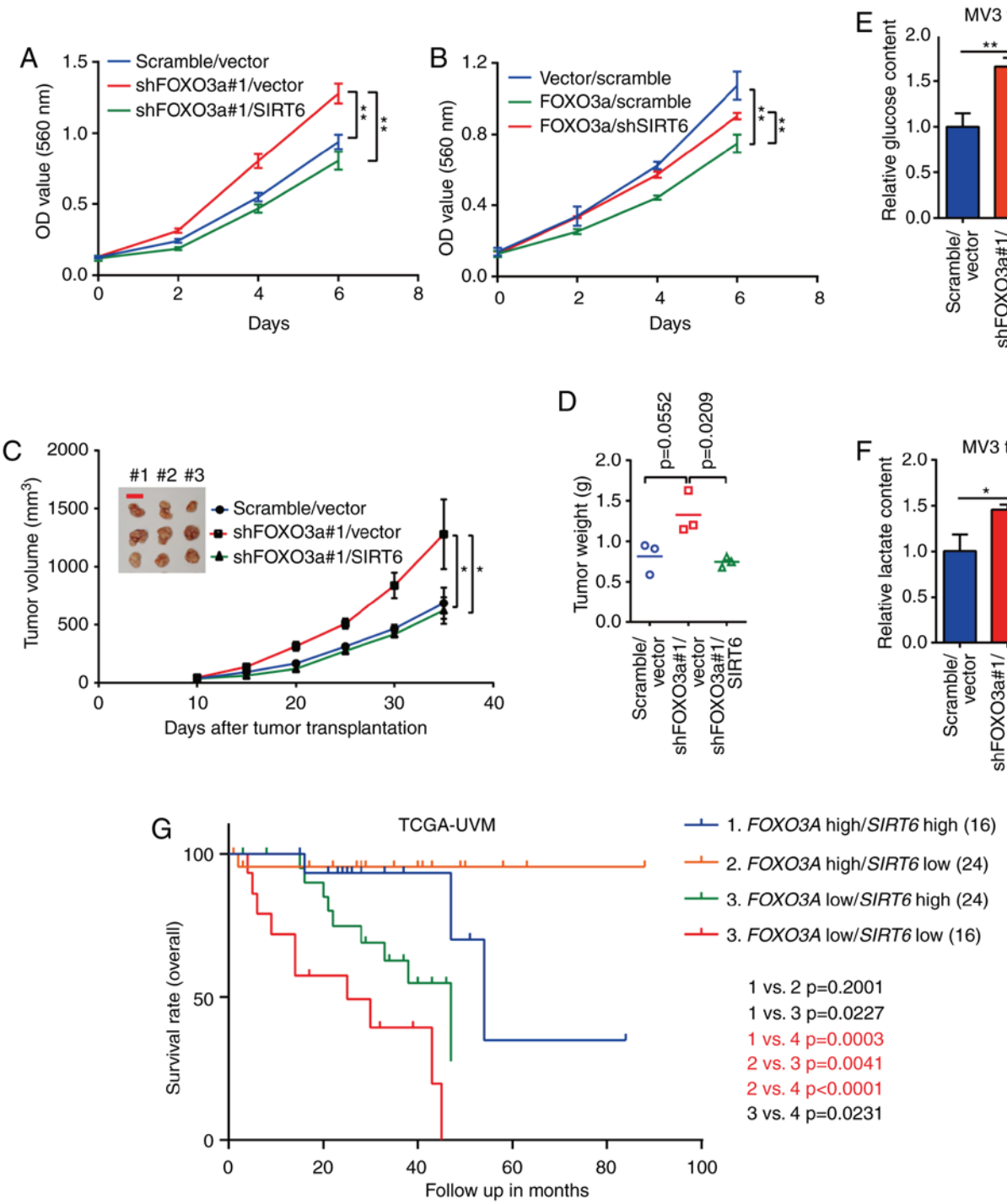

Figure 6. FOXO3a-SIRT6 axis contributes to melanoma cell viability *in vitro* and tumorigenicity *in vivo*. (A) Cell viability was determined by MTT assays in FOXO3a-silenced MV3 cells after SIRT6 overexpression. (B) Cell viability was determined by MTT assays in FOXO3a-overexpressing MV3 cells after SIRT6 silencing. (C) Tumor volume across 25 days after formation of visible tumors in BALB/c-nu mice injected MV3 cells with FOXO3a silencing and SIRT6 overexpression. The first measurements were made 10 days after injection. Scale bar, 1 cm. (D) Tumor weight at 35 days after FOXO3a-silenced MV3 cells with SIRT6 overexpression were injected into BALB/c-nu mice. (E) Relative glucose content was detected in tumors formed by FOXO3a-silenced MV3 cells with SIRT6 restoration. (F) Relative lactate content was detected using a lactate assay kit in tumors formed by FOXO3a-silenced MV3 cells with SIRT6 restoration. (G) Kaplan-Meier analysis of *FOXO3A* and *SIRT6* expression in the TCGA Ocular melanomas (project no. TCGA-UVM) dataset downloaded from the UCSC Xena (http://xena.ucsc.edu/). Groups were separated based on the median cutoff modus; a Bonferroni correction was used after the log-rank test to determine significant differences between two groups. P<0.00833 (0.05/6) was considered significant in this panel. Significant comparisons were marked as red. *P<0.05, **P<0.01, ***P<0.001. FOXO3a, forkhead box O3; SIRT6, sirtuin 6; sh, short hairpin (RNA).

investigated *in vitro*. MTT assays showed that FOXO3a silencing promoted cell viability, whereas FOXO3a overexpression inhibited cell viability (Fig. 6A and B). Furthermore, SIRT6 overexpression and silencing rescued the effects on cell viability induced by FOXO3a silencing and overexpression, respectively (Fig. 6A and B). Subsequently, a xenograft nude mouse model was employed to confirm the effect of the FOXO3a-SIRT6 axis on the growth of MV3 cells *in vivo*.

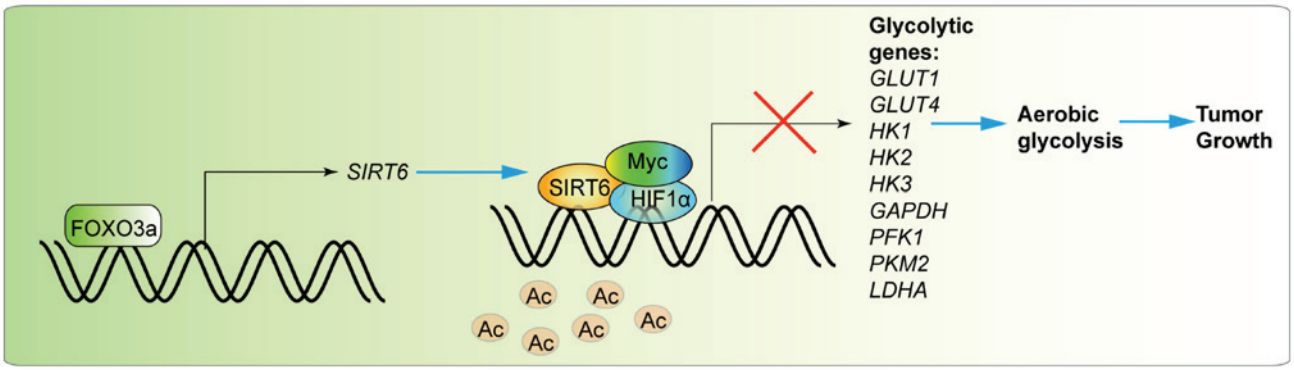

Figure 7. Model of action for the FOXO3a-SIRT6 regulatory axis in the modulation of cell metabolism in melanoma cells. Briefly, FOXO3a transcriptionally promotes the expression of *SIRT6*, which subsequently deacetylates H3K9 in the promoters of a cluster of glycolysis-associated genes, transcriptionally suppressing their expression in association with HIF1α or Myc. FOXO3a, forkhead box O3; SIRT6, sirtuin 6; HIF1α, hypoxia-inducible factor 1α; Ac, acetyl; *HK*, hexokinase; *GLUT*, glucose transporter; *PFK1*, phosphofructokinase 1; *PKM2*, pyruvate kinase isozyme 2; *LDHA*, lactate dehydrogenase A.

The results showed that FOXO3a silencing promoted tumor growth *in vivo*, whereas SIRT6 restoration rescued the effect of FOXO3a silencing (Fig. 6C and D). Then, the glucose and lactate contents of tumors were detected, and the results showed that the contents of glucose and lactate were significantly increased in FOXO3a-silenced tumors; however, this effect was attenuated by SIRT6 restoration (Fig. 6E and F). To further validate the role of the FOXO3a-SIRT6 axis using clinical data, a cohort from the TCGA melanoma database was analyzed. The results showed that FOXO3a high/SIRT6 high co-expression predicted the best overall survival rate, whereas the FOXO3a low/SIRT6 low subgroup exhibited the worst prognosis (Fig. 6G). These results indicated that the FOXO3a-SIRT6 regulatory axis is an important regulator in cellular metabolism and tumor growth of melanoma cells both *in vitro* and *in vivo*.

Discussion

Previous studies have reported that FOXO3a is a downstream factor of PI3K/AKT that inhibits the survival, growth, migration and invasion of uveal melanoma cells, as well as inducing cell cycle arrest at G1 phase and apoptosis by transcriptionally regulating the expression of its downstream genes, including Bcl-2-like protein 11, cyclin-dependent kinase inhibitor 1B, survivin and cyclin D1 (21,23,24,36). Furthermore, FOXO3a triple mutant overexpression sensitized melanoma cells to apoptosis induced by temozolomide (22). These previous indicated that FOXO3a plays important roles in the development of melanoma.

In the present study, it was found that high FOXO3a expression predicted improved prognosis for patients with melanoma. Additionally, FOXO3a expression was associated with the malignancy of melanoma. These results were consistent with previous reports. However, in addition to transcriptionally regulated genes related to cell cycle and apoptosis (21,23,24,36), there was an alternative mechanism for FOXO3a in the development of melanoma; it was observed that FOXO3a regulated aerobic glycolysis by regulating the expression of SIRT6, which is recognized as a major regulator of cellular metabolism in cancer (8).

Aerobic glycolysis is an important feature of melanoma; in normoxia, melanoma cells with varying heterogeneity typically display highly glycolytic phenotypes, in which 60-80% of glucose is metabolized into lactate (37). BRAF(V600E) oncogene, a major driver in the tumorigenesis of melanoma, has been shown to promote aerobic glycolysis (38). This highly glycolytic phenotype is characterized by high expression of glycolysis-associated genes that encode glucose transporters and enzymes involved in aerobic glycolysis. For example, in melanoma, high expression levels of glycolytic proteins such as GAPDH and PKM2 were associated with worse clinical outcome in stage III melanoma (39,40). Additionally, GLUT1 was highly expressed in melanoma tissues and revealed to enhance the metastasis of malignant melanoma cells (41). In stage IV melanomas with high serum LDH, glycolysis is the principle source of energy (42). These findings indicate that modulating aerobic glycolysis may be a promising approach to treat melanoma. In the present study, it was shown that *FOXO3A* expression in several cohorts of patient with melanoma was negatively correlated with the expression of a cluster of glycolysis-associated genes, including *HK1, HK3, PFKM, PFKFB3, PKM* and *LDHA*.

It was revealed that *FOXO3a* was positively correlated with the expression of a major glycolysis regulator, *SIRT6*, a histone deacetylase. SIRT6 can regulate the expression of various glycolysis-associated genes, including *GLUT1, PDK4, PDK1, ALDOC, PFK1, LDHB, LDHA, TPI5* and *GAPDH* by directly deacetylating histone 3 lysine 9; meanwhile, SIRT6 also represses the transcriptional activity of HIF1α and Myc, transcription factors that also regulate genes associated with glycolysis (35,43,44). The critical function of SIRT6 in the modulation of aerobic glycolysis has been reported in numerous tumors, such as breast cancer (45), urothelial carcinoma (46) and hepatocellular carcinoma (47). However, to our knowledge, the function of SIRT6-regulated glycolysis had not previously been explored in melanoma.

In the present study, it was found that FOXO3a could transcriptionally promote the expression of *SIRT6*. The detailed mechanism of FOXO3-regulated SIRT6 expression in humans varies from that previously reported in mice. In mice, the transcription factor NRF1 regulates the transcription of *SIRT6*, whereas FOXO3a only functions as a co-promoter (34). However, no binding sites for NRF1 were observed in the promoter region of the human *SIRT6* promoter. Conversely,

it was demonstrated that FOXO3a functioned as a direct transcription factor that targeted the promoter of *SIRT6*. Recently, a similar mechanism has also been reported in a study in colon cancer (48).

To elucidate the critical function of the FOXO3a-SIRT6 axis in the regulation of glycolysis and tumor growth in melanoma, SIRT6 was overexpressed in FOXO3a-silenced MV3 cells and SIRT6 was knocked down in FOXO3a-overexpressing MV3 cells. Then, glucose uptake and consumption, lactate production, LDH activity, glycolytic gene expression and cell viability were evaluated *in vitro*, and tumor growth was investigated *in vivo*. The results showed that the effects of altered FOXO3a expression could be rescued by inverse manipulations of SIRT6 expression, indicating that the FOXO3a-SIRT6 axis played a pivotal role in the modulation of cell metabolism and tumor growth. However, the function of this axis may vary in different types of cancers and under different conditions. For example, GLUT1 expression is reduced in the absence of FOXO3a in glioma cells under serum starvation (49), implying that FOXO3a has a more complex role in the regulation of cell metabolism and cell survival.

In conclusion, the present study identified a novel mechanism for FOXO3a in the suppression of melanoma development. FOXO3a transcriptionally promoted the expression of SIRT6, which subsequently suppressed the expression of a number of glycolysis-associated genes (Fig. 7). The FOXO3a-SIRT6 regulatory axis serves an important role in modulating cellular metabolism, thereby affecting cancer development *in vitro* and *in vivo*. The present findings indicated that the FOXO3a-SIRT6 axis may be a therapeutic target for the treatment of melanoma.

Acknowledgements

We thank Mr. Gaichao Zhao (State Key Laboratory of Silkworm Genome Biology, Southwest University) for his contributions to the revision of this manuscript.

Funding

This work was supported by the Project Funded by Chongqing Special Postdoctoral Science Foundation (grant no. XmT2018080), the National Key Research and Development Program of China (grant nos. 2017YFC1308600 and 2016YFC1302204), the National Natural Science Foundation of China (grant nos. 81672502, 31672496 and 81902664), the Fundamental Research Funds for the Central Universities (grant no. XDJK2019C013), and the Research and Innovation Project of Graduate Students in Chongqing (grant no. CYS19136).

Availability of data and materials

The datasets used and/or analyzed during the current study are available from the corresponding author on reasonable request.

Authors' contributions

ZD performed the experiments, acquired the data and drafted the manuscript. JY, LL, LT and PS performed molecular biological experiments. JZ, XZ and LG analyzed the data and performed statistical analysis. ZW and HC conceived and designed the study, and reviewed/revised the manuscript, figures and tables. All authors read and approved the final manuscript.

Ethics approval and consent to participate

The animal experiments in the current study were approved and supervised by the Institutional Animal Care and Use Committees of the Southwest University (permit no. IACUC-20190402-02) and the Experimental Animal Care and Use Committees of the Institute of Sericulture and Systems Biology. The study was performed according to the Laboratory Animal Management Regulations and the Measures of Chongqing Municipality on the Management of Experimental Animals.

Patient consent for publication

Not applicable.

Competing interests

The authors declare that they have no competing interests.

References

1. Dimitriou F, Krattinger R, Ramelyte E, Barysch MJ, Micaletto S, Dummer R and Goldinger SM: The World of melanoma: Epidemiologic, genetic, and anatomic differences of melanoma across the globe. Curr Oncol Rep 20: 87, 2018.
2. Gray-Schopfer V, Wellbrock C and Marais R: Melanoma biology and new targeted therapy. Nature 445: 851-857, 2007.
3. Hanahan D and Weinberg RA: Hallmarks of cancer: The next generation. Cell 144: 646-674, 2011.
4. Cantor JR and Sabatini DM: Cancer cell metabolism: One hallmark, many faces. Cancer Discov 2: 881-898, 2012.
5. Vander Heiden MG, Cantley LC and Thompson CB: Understanding the Warburg effect: The metabolic requirements of cell proliferation. Science 324: 1029-1033, 2009.
6. Courtnay R, Ngo DC, Malik N, Ververis K, Tortorella SM and Karagiannis TC: Cancer metabolism and the Warburg effect: The role of HIF-1 and PI3K. Mol Biol Rep 42: 841-851, 2015.
7. Dong Z and Cui H: Epigenetic modulation of metabolism in glioblastoma. Semin Cancer Biol 57: 45-51, 2019.
8. Zhu S, Dong Z, Ke X, Hou J, Zhao E, Zhang K, Wang F, Yang L, Xiang Z and Cui H: The roles of sirtuins family in cell metabolism during tumor development. Semin Cancer Biol 57: 59-71, 2019.
9. Gatenby RA and Gillies RJ: Why do cancers have high aerobic glycolysis? Nat Rev Cancer 4: 891-899, 2004.
10. Paik JH, Kollipara R, Chu G, Ji H, Xiao Y, Ding Z, Miao L, Tothova Z, Horner JW, Carrasco DR, *et al*: FoxOs are lineage-restricted redundant tumor suppressors and regulate endothelial cell homeostasis. Cell 128: 309-323, 2007.
11. Yadav RK, Chauhan AS, Zhuang L and Gan B: FoxO transcription factors in cancer metabolism. Semin Cancer Biol 50: 65-76, 2018.
12. Hornsveld M, Dansen TB, Derksen PW and Burgering BMT: Re-evaluating the role of FOXOs in cancer. Semin Cancer Biol 50: 90-100, 2018.
13. Ma Z, Xin Z, Hu W, Jiang S, Yang Z, Yan X, Li X, Yang Y and Chen F: Forkhead box O proteins: Crucial regulators of cancer EMT. Semin Cancer Biol 50: 21-31, 2018.
14. Dong Z, Zhong X, Lei Q, Chen F and Cui H: Transcriptional activation of SIRT6 via FKHRL1/FOXO3a inhibits the Warburg effect in glioblastoma cells. Cell Signal 60: 100-113, 2019.
15. Shukla S, Shukla M, Maclennan GT, Fu P and Gupta S: Deregulation of FOXO3A during prostate cancer progression. Int J Oncol 34: 1613-1620, 2009.
16. Herzog CR, Blake DC Jr, Mikse OR, Grigoryeva LS and Gundermann EL: FoxO3a gene is a target of deletion in mouse lung adenocarcinoma. Oncol Rep 22: 837-843, 2009.

17. Jiang L, Cao XC, Cao JG, Liu F, Quan MF, Sheng XF and Ren KQ: Casticin induces ovarian cancer cell apoptosis by repressing FoxM1 through the activation of FOXO3a. Oncol Lett 5: 1605-1610, 2013.
18. Yu Y, Peng K, Li H, Zhuang R, Wang Y, Li W, Yu S, Liang L, Xu X and Liu T: SP1 upregulated FoxO3a promotes tumor progression in colorectal cancer. Oncol Rep 39: 2235-2242, 2018.
19. Ikeda JI, Wada N, Nojima S, Tahara S, Tsuruta Y, Oya K and Morii E: ID1 upregulation and FoxO3a downregulation by epstein-barr virus-encoded LMP1 in Hodgkin's lymphoma. Mol Clin Oncol 5: 562-566, 2016.
20. Ferber EC, Peck B, Delpuech O, Bell GP, East P and Schulze A: FOXO3a regulates reactive oxygen metabolism by inhibiting mitochondrial gene expression. Cell Death Differ 19: 968-979, 2012.
21. Yu T, Ji J and Guo YL: MST1 activation by curcumin mediates JNK activation, Foxo3a nuclear translocation and apoptosis in melanoma cells. Biochem Biophys Res Commun 441: 53-58, 2013.
22. Egger ME, McNally LR, Nitz J, McMasters KM and Gomez-Gutierrez JG: Adenovirus-mediated FKHRL1/TM sensitizes melanoma cells to apoptosis induced by temozolomide. Hum Gene Ther Clin Dev 25: 186-195, 2014.
23. Hilmi C, Larribere L, Deckert M, Rocchi S, Giuliano S, Bille K, Ortonne JP, Ballotti R and Bertolotto C: Involvement of FKHRL1 in melanoma cell survival and death. Pigment Cell Melanoma Res 21: 139-146, 2008.
24. Yan F, Liao R, Farhan M, Wang T, Chen J, Wang Z, Little PJ and Zheng W: Elucidating the role of the FoxO3a transcription factor in the IGF-1-induced migration and invasion of uveal melanoma cancer cells. Biomed Pharmacother 84: 1538-1550, 2016.
25. Livak KJ and Schmittgen TD: Analysis of relative gene expression data using real-time quantitative PCR and the 2(-Delta Delta C(T)) method. Methods 25: 402-408, 2001.
26. Wang M, Liu Y, Zou J, Yang R, Xuan F, Wang Y, Gao N and Cui H: Transcriptional co-activator TAZ sustains proliferation and tumorigenicity of neuroblastoma by targeting CTGF and PDGF-β. Oncotarget 6: 9517-9530, 2015.
27. Yang R, Yi L, Dong Z, Ouyang Q, Zhou J, Pang Y, Wu Y, Xu L and Cui H: Tigecycline inhibits glioma growth by regulating miRNA-199b-5p-HES1-AKT pathway. Mol Cancer Ther 15: 421-429, 2016.
28. He J, Zhao Y, Zhao E, Wang X, Dong Z, Chen Y, Yang L and Cui H: Cancer-testis specific gene OIP5: A downstream gene of E2F1 that promotes tumorigenesis and metastasis in glioblastoma by stabilizing E2F1 signalling. Neuro Oncol 20: 1173-1184, 2018.
29. Johnson DB and Puzanov I: Treatment of NRAS-mutant melanoma. Curr Treat Options Oncol 16: 15, 2015.
30. Willcox BJ, Donlon TA, He Q, Chen R, Grove JS, Yano K, Masaki KH, Willcox DC, Rodriguez B and Curb JD: FOXO3A genotype is strongly associated with human longevity. Proc Natl Acad Sci USA 105: 13987-13992, 2008.
31. Hirvonen K, Laivuori H, Lahti J, Strandberg T, Eriksson JG and Hackman P: SIRT6 polymorphism rs117385980 is associated with longevity and healthy aging in Finnish men. BMC Med Genet 18: 41, 2017.
32. Tao R, Xiong X, DePinho RA, Deng CX and Dong XC: FoxO3 transcription factor and Sirt6 deacetylase regulate low density lipoprotein (LDL)-cholesterol homeostasis via control of the proprotein convertase subtilisin/kexin type 9 (Pcsk9) gene expression. J Biol Chem 288: 29252-29259, 2013.
33. Tao R, Xiong X, DePinho RA, Deng CX and Dong XC: Hepatic SREBP-2 and cholesterol biosynthesis are regulated by FoxO3 and Sirt6. J Lipid Res 54: 2745-2753, 2013.
34. Kim HS, Xiao C, Wang RH, Lahusen T, Xu X, Vassilopoulos A, Vazquez-Ortiz G, Jeong WI, Park O, Ki SH, *et al*: Hepatic-specific disruption of SIRT6 in mice results in fatty liver formation due to enhanced glycolysis and triglyceride synthesis. Cell Metab 12: 224-236, 2010.
35. Zhong L, D'Urso A, Toiber D, Sebastian C, Henry RE, Vadysirisack DD, Guimaraes A, Marinelli B, Wikstrom JD, Nir T, *et al*: The histone deacetylase Sirt6 regulates glucose homeostasis via Hif1alpha. Cell 140: 280-293, 2010.
36. Yan F, Liao R, Lin S, Deng X, Little PJ and Zheng W: Forkhead box protein O3 suppresses uveal melanoma development by increasing the expression of Bcl2like protein 11 and cyclindependent kinase inhibitor 1B. Mol Med Rep 17: 3109-3114, 2018.
37. Scott DA, Richardson AD, Filipp FV, Knutzen CA, Chiang GG, Ronai ZA, Osterman AL and Smith JW: Comparative metabolic flux profiling of melanoma cell lines: Beyond the Warburg effect. J Biol Chem 286: 42626-42634, 2011.
38. Hall A, Meyle KD, Lange MK, Klima M, Sanderhoff M, Dahl C, Abildgaard C, Thorup K, Moghimi SM, Jensen PB, *et al*: Dysfunctional oxidative phosphorylation makes malignant melanoma cells addicted to glycolysis driven by the (V600E)BRAF oncogene. Oncotarget 4: 584-599, 2013.
39. Falkenius J, Lundeberg J, Johansson H, Tuominen R, Frostvik-Stolt M, Hansson J and Egyhazi Brage S: High expression of glycolytic and pigment proteins is associated with worse clinical outcome in stage III melanoma. Melanoma Res 23: 452-460, 2013.
40. Najera L, Alonso-Juarranz M, Garrido M, Ballestín C, Moya L, Martínez-Díaz M, Carrillo R, Juarranz A, Rojo F, Cuezva JM and Rodríguez-Peralto JL: Prognostic implications of markers of the metabolic phenotype in human cutaneous melanoma. Br J Dermatol 181: 114-127, 2019.
41. Koch A, Lang SA, Wild PJ, Gantner S, Mahli A, Spanier G, Berneburg M, Müller M, Bosserhoff AK and Hellerbrand C: Glucose transporter isoform 1 expression enhances metastasis of malignant melanoma cells. Oncotarget 6: 32748-32760, 2015.
42. Ho J, de Moura MB, Lin Y, Vincent G, Thorne S, Duncan LM, Hui-Min L, Kirkwood JM, Becker D, Van Houten B and Moschos SJ: Importance of glycolysis and oxidative phosphorylation in advanced melanoma. Mol Cancer 11: 76, 2012.
43. Sebastián C, Zwaans BM, Silberman DM, Gymrek M, Goren A, Zhong L, Ram O, Truelove J, Guimaraes AR, Toiber D, *et al*: The histone deacetylase SIRT6 is a tumor suppressor that controls cancer metabolism. Cell 151: 1185-1199, 2012.
44. Kleszcz R, Paluszczak J, Krajka-Kuźniak V and Baer-Dubowska W: The inhibition of c-MYC transcription factor modulates the expression of glycolytic and glutaminolytic enzymes in FaDu hypopharyngeal carcinoma cells. Adv Clin Exp Med 27: 735-742, 2018.
45. Choe M, Brusgard JL, Chumsri S, Bhandary L, Zhao XF, Lu S, Goloubeva OG, Polster BM, Fiskum GM, Girnun GD, *et al*: The RUNX2 transcription factor negatively regulates SIRT6 expression to alter glucose metabolism in breast cancer cells. J Cell Biochem 116: 2210-2226, 2015.
46. Wu M, Dickinson SI, Wang X and Zhang J: Expression and function of SIRT6 in muscle invasive urothelial carcinoma of the bladder. Int J Clin Exp Pathol 7: 6504-6513, 2014.
47. Feng XX, Luo J, Liu M, Yan W, Zhou ZZ, Xia YJ, Tu W, Li PY, Feng ZH and Tian DA: Sirtuin 6 promotes transforming growth factor-β1/H2O2/HOCl-mediated enhancement of hepatocellular carcinoma cell tumorigenicity by suppressing cellular senescence. Cancer Sci 106: 559-566, 2015.
48. Zhang Y, Nie L, Xu K, Fu Y, Zhong J, Gu K and Zhang L: SIRT6, a novel direct transcriptional target of FoxO3a, mediates colon cancer therapy. Theranostics 9: 2380-2394, 2019.
49. Brucker DP, Maurer GD, Harter PN, Rieger J and Steinbach JP: FOXO3a orchestrates glioma cell responses to starvation conditions and promotes hypoxia-induced cell death. Int J Oncol 49: 2399-2410, 2016.